

**Material:** Ferritic Steel: Eurofer 97  
**Property:** Time (h) versus Strain (%)  
**Condition:** Irradiated  
**Data:** Experimental

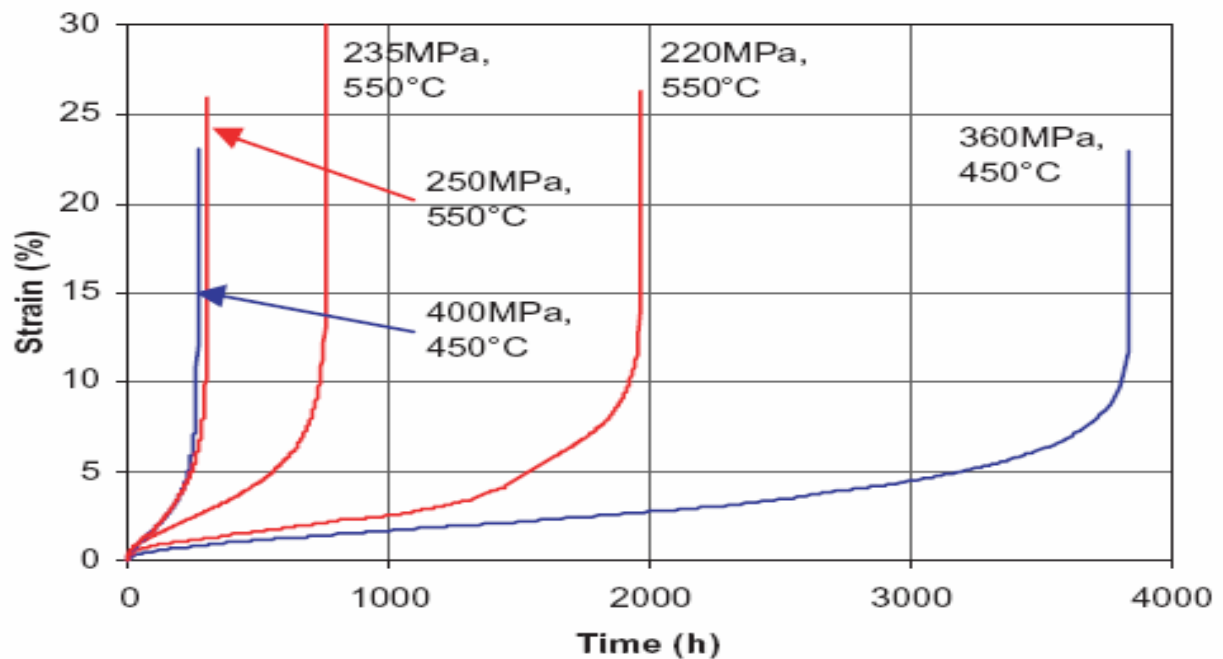


Fig. 2. Creep tests for Eurofer 97 1100 °C HIP joints.

**Source:**

Journal of Nuclear Materials, 329-333, (2004), 133-140

**Title of paper (or report) this figure appeared in:**

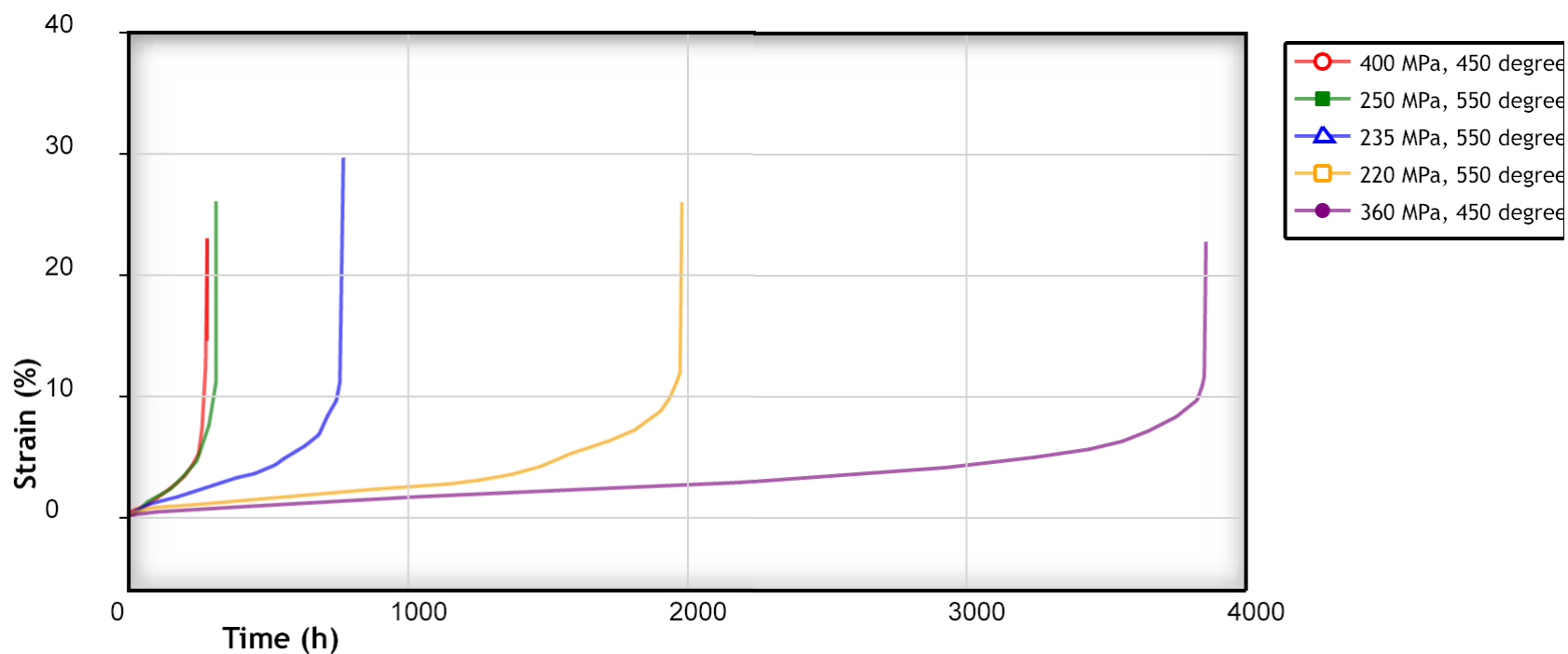
The manufacturing technologies of the European breeding blankets

**Author of paper or graph:**

A. Cardella, E. Rigal, L. Bedel, Ph. Bucci, J. Fiek, L. Forest, L. V. Boccaccini,  
E. Diegele, L. Giancarli, S. Hermsmeyer, G. Janeschitz, R. Lässer,  
A. Li Puma, J. D. Lulewicz, A. Möslang, Y. Poitevin, E. Rabaglino

**Caption:**

Creep tests for Eurofer 97 1100 °C HIP joints.



Creep tests for Eurofer 97 1100 °C HIP joints.

**Reference:**

**Author:** A. Cardella, E. Rigal, L. Bedel, Ph. Bucci, J. Fiek, et. all

**Title:** The manufacturing technologies of the European breeding blankets

**Source:** Journal of Nuclear Materials, 2004, Volume 329-333, Page 133-140, [\[PDF\]](#)

[View Data](#)

[Author Comments](#)

**Plot Format:**

**Y-Scale:** ☒ linear ☐ log ☐ ln

**X-Scale:** ☒ linear ☐ log ☐ ln

[Update](#)

[Close Window](#)

## The manufacturing technologies of the European breeding blankets

A. Cardella <sup>a,\*</sup>, E. Rigal <sup>b</sup>, L. Bedel <sup>b</sup>, Ph. Bucci <sup>b</sup>, J. Fiek <sup>c</sup>,  
L. Forest <sup>d</sup>, L.V. Boccaccini <sup>c</sup>, E. Diegele <sup>a</sup>, L. Giancarli <sup>d</sup>,  
S. Hermesmeyer <sup>c</sup>, G. Janeschitz <sup>c</sup>, R. Lässer <sup>a</sup>, A. Li Puma <sup>d</sup>,  
J.D. Lulewicz <sup>d</sup>, A. Möslang <sup>c</sup>, Y. Poitevin <sup>d</sup>, E. Rabaglini <sup>c</sup>

<sup>a</sup> EFDA CSU, Boltzmannstrasse 2, D-85748 Garching, Germany

<sup>b</sup> CEA-Grenoble, 17 rue des Martyrs, 38054 Grenoble cedex 9, France

<sup>c</sup> Forschungszentrum Karlsruhe, P.O. Box 3640, D-76021 Karlsruhe, Germany

<sup>d</sup> CEA-Saclay, 91191 Gif-sur-Yvette, France

### Abstract

In the European Union, the basic manufacturing technologies have been selected for the two reference DEMO breeding blanket concepts: the helium cooled pebble bed and the helium cooled lithium lead. These technologies have been tested in the past years on small-scale samples and mock-ups, are presently under further development, and are now being adapted to the evolution of the two concepts. After successful testing they will be directly applied and verified on the test blanket modules, which are designed to be DEMO relevant and will be installed and tested in ITER.

© 2004 Elsevier B.V. All rights reserved.

### 1. Introduction

The main objective of the present European R&D on breeder blankets (BBs) is the development of test blanket modules (TBMs) to be installed and tested in ITER, which are representative of two reference DEMO BB concepts: the helium cooled pebble bed (HCPB) and the helium cooled lithium lead (HCLL). Both BB concepts have a common architectural structure and share as much as possible the R&D activities for the TBM metallic structures.

The basic manufacturing technologies for the DEMO and TBM structures have been selected and tested in the past years mostly on small-scale samples and mock-ups. These technologies are presently under further development and will be used in the near future for the

manufacturing of large-scale prototypical mock-ups of the TBMs. They will finally be directly applied to and verified on the TBMs.

In addition to the R&D for the manufacturing of the structural parts, a considerable R&D effort for the HCPB is devoted to the production of the ceramic breeder ( $\text{Li}_4\text{SiO}_4$  or  $\text{Li}_2\text{TiO}_3$ ) and neutron multiplier (beryllium or beryllium alloy) pebble beds, for which semi-industrial manufacturing processes have been developed. For the HCLL a specific activity is focused on the development of anti-corrosion and tritium-permeation barrier coatings; no specific R&D has been instead performed so far on the production of the breeder/multiplier material (liquid  $\text{PbLi}$ ), because it is expected that for near future needs this can directly be purchased at the required purity.

### 2. The breeder blanket concepts

The DEMO BB [1–3] is designed in modules ( $\sim 2 \times 2 \times 1$  m assumed as typical), cooled by helium at

\* Corresponding author. Tel.: +49-89 3299 4100; fax: +49-89 3299 4198.

E-mail address: [antonio.cardella@tech.efda.org](mailto:antonio.cardella@tech.efda.org) (A. Cardella).

8 MPa. Each module has a structure formed by a steel box reinforced by a grid of poloidal/radial and toroidal/radial stiffening plates and mainly consists of:

- a U-shaped steel shell, 29 mm thick for the HCPB, 25 mm for the HCLL, with internal rectangular cooling channels of  $18 \times 18 \text{ mm}^2$  cross-section for the HCPB and  $15.6 \times 14 \text{ mm}^2$  for the HCLL both with 6 mm ribs between channels. The front part forms the first wall (FW) and the lateral sides form the side walls of the box,
- two top and bottom, internally cooled closure plates caps with thickness and channels similar to the FW,
- the grid of stiffening plates (SP) with small internal rectangular cooling channels, with a thickness between 6.5 for the HCLL and 11 mm for the HCPB,
- a back-wall (BW) made-up of four steel plates (plus two for the HCPB tritium purge system), which is also used as the manifold/flow distributor for the blanket fluids (helium as coolant for both HCLL and HCPB, helium as purge gas for the HCPB and PbLi for the HCLL),
- the module main inlet outlet headers.

The SPs inside the box form square radial cells of about 200 mm side, making the box able to withstand the coolant pressure in accidental conditions. The joints of each group of four stiffening plates form on the rear side a cross that is fixed to the back-walls in order to provide helium distribution. Inside the stiffening grid are inserted the different breeder units (BU) for the HCLL and HCPB BBs.

The HCPB BU uses thin (5 mm) steel plates with internal cooling channels to separate beds of ceramic breeder and of beryllium pebbles. These plates are mechanically supported and fed with coolant from a breeder unit back plate. Both types of pebble beds are purged by a slow helium flow to supply the fuel cycle and keep the tritium inventory low.

The HCLL BU consists of a poloidal array of 5 parallel cooling plates (CPs) (similar to the SPs), connected to a back-plate. The PbLi is cooled by the CPs and laterally by the SPs. Ad hoc slots are derived at the edges of the CPs and SPs in order to allow a slow flow of the PbLi following a meandering path from the top to the bottom of the BB module.

### 3. The manufacturing technologies for the blanket structures

The reference structural material for the EU BB is EUROFER, a reduced-activation-ferritic-martensitic (RAFM) steel that has been developed and characterized for the near-term DEMO BB [4–7] in the EU materials development program.

From the description above it is evident that the concepts rely heavily on plates with internal cooling channels. The main technologies needed to fabricate the blanket are: (1) cutting and machining of semi-finished products; (2) joining of parts, particularly to produce the plates with internal channels and to build up the blanket structure; (3) bending of cooling plates as a mean of avoiding as far as possible fusion welds close to the FW and; (4) heat treatment of the joints to improve their mechanical properties.

Of these steps, joining and heat treatment together are the key technologies that determine the mechanical strength of the blanket, the ductile to brittle transition temperature (DBTT) relevant in a nuclear environment, and the potential for compact design. The present paper describes these technologies that have been a focus of the EU programme. Two joining principles are applied. The main manufacturing process for the plates is hot isostatic pressing (HIP) that involves diffusion processes in the joining area. Fusion welding processes such as electron beam welding (EBW), tungsten inert gas welding (TIG) or laser welding are nonetheless also required particularly for assembling/joining HIPed parts, closures and fittings and the external connections of the blanket modules.

#### 3.1. HIP joining techniques

HIP involves heating encapsulated parts at high temperature in a high pressure atmosphere, which results in the collapse and closure of holes, gaps and porosities of all kinds through creep and diffusion mechanisms. HIP is used to achieve complex shape components by solid phase welding (diffusion welding) elemental, simple parts. It is of utmost importance to achieve very good joint mechanical properties because the joints may be located in areas of the modules, which are either highly thermally stressed during operation or highly mechanically stressed in faulted conditions. It is equally important that the process does not affect the properties of the base material. HIP has the potential to produce joints of near base material quality even under irradiation.

##### 3.1.1. HIP parameters and post-HIP heat treatment

It is very important to achieve grain boundary mobility across the joint otherwise mechanical properties as good as those of the base material cannot be expected [9]. This joint ‘polygonisation’ may be hindered in two main instances:

- hindering of grain boundary mobility by surface impurities; experimental work at FZK and CEA has shown that the best surface preparation consists of dry machining followed by careful solvent cleaning [10];

- insufficient HIP parameters (temperature, pressure and time-to-temperature). Eurofer grain growth begins between 1050 and 1100 °C [6,11]. This suggests choosing such high HIP temperatures. However, data are less clear for the lower limit e.g. of temperature which would be attractive for achieving full joint strength without excessive base material grain growth.

The two options currently considered in Europe target the extremes of the feasible temperature range. In the CEA approach, a one step HIP at 1100 °C is applied. Because a small grain size is favourable to base material mechanical properties, particularly the DBTT [7], this approach requires a post-HIP heat treatment (PHHT) that includes austenitisation at moderate temperature in order to reduce the grain size. HIP temperatures in the FZK approach are chosen between 980 and 1050 °C. Results at 980 °C suggest that sufficient joint quality is achieved while small grains are preserved, avoiding the need for including austenitisation in the PHHT (that consists only of tempering at 750 °C).

As far as quenching is concerned, the minimum cooling rate to achieve a full martensitic transformation in Eurofer (for an austenitisation at 980 °C) is 5 K/min [6]. Other authors have determined a slightly lower value, i.e. 3.5 K/min [11], but for a different heat with a probably different grain size. From the manufacturing point of view uncertainties linked to temperature homogeneity leads to imposing a minimum value of 10 K/min, which is easily achieved in modern HIP devices.

### 3.1.2. Joint mechanical properties

In a screening phase the quality of the joints has been first evaluated with basic tests, namely room temperature tensile and impact toughness testing. However it is well known that tensile testing highlights only basic flaws in the joint [9,12] and much emphasis has been put on impact toughness testing.

Eurofer 97 discs, 100 mm diameter, were machined with various surface roughness, cleaned with a mixture of solvents and inserted in a SS304L canister. The canister was outgassed at 250 °C for several tens of hours, sealed and HIPed for 2 h at 1100 °C, 100 MPa. The PHHT was 2 h at 950 °C, air cooling + tempering 2 h at 750 °C. KLST impact test results are given in Table 1. Impact toughness close to or equal to that of the forged material, i.e. 9.5 J is achieved. Better results are obtained with smooth surfaces, not because pores persist at interfaces resulting from rough surfaces, but most probably because contamination is more easily removed. These results show that a mean roughness lower than 1.6 µm is desirable. It was verified that the joint DBTT is identical to that of the base material. Due to the low austenitisation temperature during PHHT, the DBTT is

Table 1

KLST impact toughness of Eurofer 97 HIP joint (see text for details)

| Sample            | Joint A    | Joint B   | Joint C   |
|-------------------|------------|-----------|-----------|
| Machining process | Grinding   | Milling   | Milling   |
| Mean roughness    | 0.3 µm     | 1.6 µm    | 6.3 µm    |
| KLST (J)          | 10.1 ± 0.4 | 9.7 ± 0.5 | 8.6 ± 0.7 |

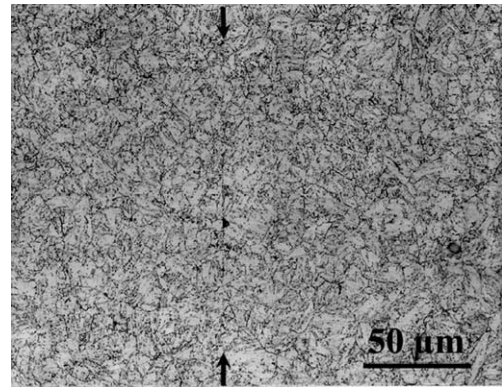


Fig. 1. Microstructure of a Eurofer 97 1100 °C HIP joint.

actually even lower than that of the forged material, the latter having being austenitised at 980 °C.

The microstructure of a joint achieved from specimens milled to 0.8 µm mean roughness is given on Fig. 1: the interface is hardly visible. A full mechanical characterisation of the joints was made, including creep (Fig. 2), low cycle fatigue (Fig. 3) and fracture toughness testing. In all tests the rupture never occurred at the joint. However, some cavities were found at the joint in creep tested specimens. These findings have to be confirmed in irradiated conditions.

The claims for high quality EUROFER HIP joints at temperatures as low as 980 °C are supported by parameter optimisation experiments on a circular bonding zone seal-welded by EBW prior to HIP. Parameters were 2 µm maximum roughness and 3 h bonding at 980 and 1050 °C, 50 MPa. Tensile properties are identical to the base material. Impact energies are about 90%.

In the near future EU materials R&D the issue of a comprehensive set of HIP joints mechanical properties (fatigue, creep, fracture toughness) is planned for a full qualification.

### 3.1.3. First wall fabrication

The FW may be achieved using different fabrication sequences.

The two-step HIP of the first wall from two grooved plates (Table 2, first row) has been studied at FZK with three small 90×90 mm<sup>2</sup> EUROFER mock-ups [13].

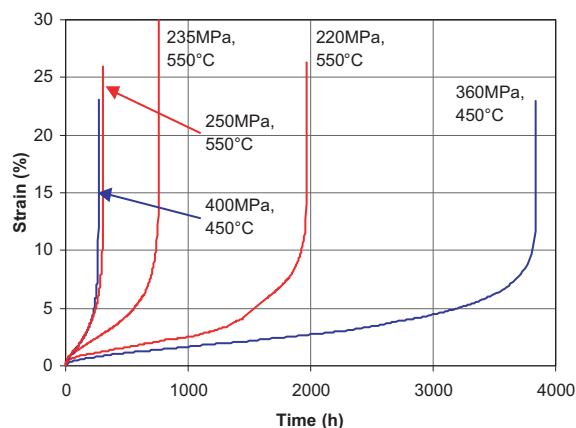


Fig. 2. Creep tests for Eurofer 97 1100 °C HIP joints.

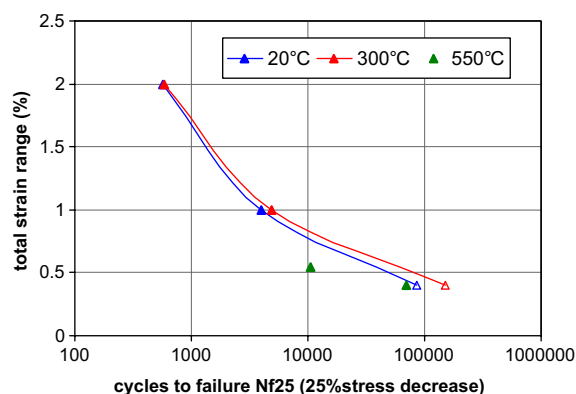


Fig. 3. Low cycle fatigue test results for Eurofer 97 HIP joints. Open symbols stand for interrupted tests (no failure).

In order to avoid the collapse of the channels, molybdenum alloy stiffening plates are encapsulated with the grooved plates in a canister evacuated and sealed, then a first low pressure HIP cycle is applied to the canister ( $\sim 10$  MPa, 1050 °C, 2 h). The objective of this first HIP is to seal the periphery of the interface (fusion welding is an alternative process for this step). Then, the canister and the Mo plates are removed and the channels are opened by drilling. The FW is further HIPed at high pressure to achieve full bonding (200 MPa, 1050 °C, 3 h). Finally, the FW is tempered for 2 h at 750 °C. Mechanical room-temperature tests of the joint show that tensile properties in the range of the base material are achieved, and that notch impact tests reach up to 85% of the base material.

In a parallel development, a semi-size blanket box mock-up using MANET ferritic martensitic steel [8] demonstrated FW bending and welding of cooling plates to the box.

Table 2  
Scheme of FW fabrication processes

|                           |  |
|---------------------------|--|
| 2-Steps<br>HIP            |  |
| HIP<br>forming            |  |
| Rectan-<br>gular<br>tubes |  |

Two other solutions based on a single high pressure HIP at 1100 °C have been studied by CEA. The joint geometry is more complex than above. First, the so-called 'HIP-forming' process involves the insertion of round tubes in the rectangular grooves (Table 2 second row). The ends of the tubes are welded to the plates but the tubes are not closed. During HIP the tubes expand and conform to the grooves. Stiffening plates are necessary to avoid the grooved plates deformation. Second, the 'rectangular tube (RT) process' (Table 2 third row) involves the diffusion welding of RTs and cover plates. With this process there is no need for stiffening plates since there is no tube expansion. Furthermore, RTs and cover plates may be bent before HIP, which opens the possibility to manufacture module skeleton before adding the FW. The RT process is still under development.

A view of a 3-channels mock up before and after HIP-forming, bending and machining is given in Fig. 4. The mechanical properties of the joints are given in Table 3. The tensile specimens broke away from the interface and they fulfil base material specifications [14]. Impact specimens opened at the interface but they did not break entirely. Nevertheless, impact toughness values are lower than those measured on small samples, which are easier to handle for surface preparation (Table 1). Impact toughness values in the bend were similar.

#### 3.1.4. Cooling/stiffening plates fabrication

Due to the small channel dimensions and sharp channel turns, the two-step HIP is considered to be the most attractive solution for these components. The fabrication is largely identical with the procedure for the FW.

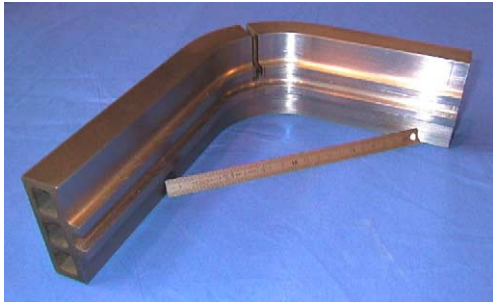


Fig. 4. FW mock up manufactured by HIP forming (top: parts before HIP; bottom, mock up after HIP, bending and machining).

### 3.2. Fusion welding

Fusion welding of RAFM steels has been developed at CEA and FZK. The objective is to provide data concerning the operational and metallurgy aspects of welds made with the TIG, EB and laser welding processes [15–17]. The influence of the post-welding heat treatment (PWHT) on the tensile and impact toughness properties is another important issue, as well as Eurofer/stainless steel 316LN welding which is required for the connection of the TBMs to the ITER supply systems [18].

The thickness of welds studied so far at CEA ranges from 1.5 to 24 mm. Macrographs of welds achieved with TIG, EB and laser processes are shown in Figs. 5–7. Three zones can be distinguished: BM (base metal), HAZ (heat affected zone) and WZ (welded zone). Non-destructive controls and the metallurgical analysis of these welds indicate that Eurofer is not sensitive to cracking and has good weldability. For these welding conditions, preheating is not required before welding.

The WZ microstructure of a 24 mm thick, single U butt weld after PWHT at 740 °C for 2.5 h is shown in Fig. 8 (TIG process). The WZ is composed mainly of martensite; laths are bordered with very fine carbides. Tensile properties are shown in Table 4: for each test temperature, three tensile specimens localized in the root, the middle and the top of the weld were machined transversally and longitudinally. After PWHT, the HV1 hardness of the HAZ decreases from 200 (close to the BM) and 340 (close to the WZ) down to 175 and 270, respectively. As far as the WZ hardness is concerned, it varies from 340 (close to HAZ) to 400 HV1 (middle of

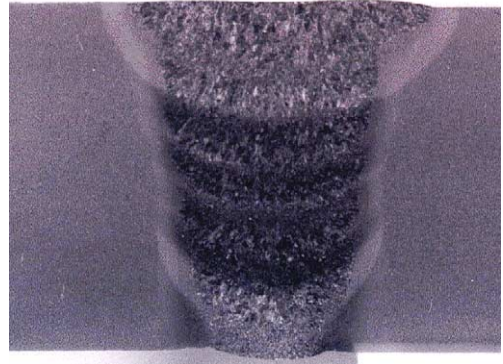


Fig. 5. Macrograph of a Eurofer plate TIG weld, 24 mm thick.

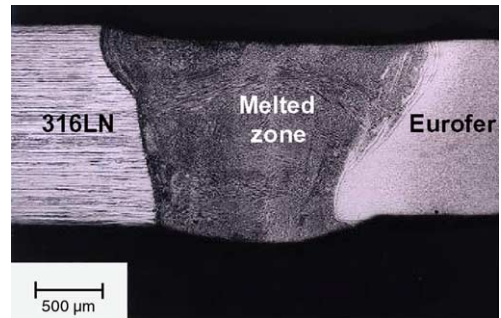


Fig. 6. Macrograph of a Eurofer/316LN tube EB weld, 1.5 mm thick.

the seam) in the as-welded condition and decreases to 260–275 after PWHT. As a result, the yield strength and the maximum stress of the WZ is rather high. A higher PWHT temperature would be required to soften further the WZ, but this would soften too much the BM. It must be noted also that the properties in the transverse and longitudinal direction are close to each other. As expected, the root is somewhat softer than the top of the seam.

In the blanket modules defect free welds are difficult to obtain so it cannot be excluded that undetected defects remain. The feasibility of an improvement of the weld quality by means of post-weld HIP has been assessed [19]. Two kinds of TIG weld defects (porosity and lack of fusion) have been intentionally produced. In both cases, the defects were located at mid-height of the seam, above sound root passes and beneath sound filling

Table 3

Room temperature mechanical properties of plate/plate joints machined from the mock up shown in Fig. 4

| Tensile                                 | KLST                                 |
|---|--------------------------------------|
| $\sigma_y$ 0.2% = 528 MPa; Rm = 642 MPa | 7.3 ± 0.3 J (10 val.)                |
| UE = 6.3%, TE = 16.5%                   | [11.1 ± 0.2 J for the base material] |



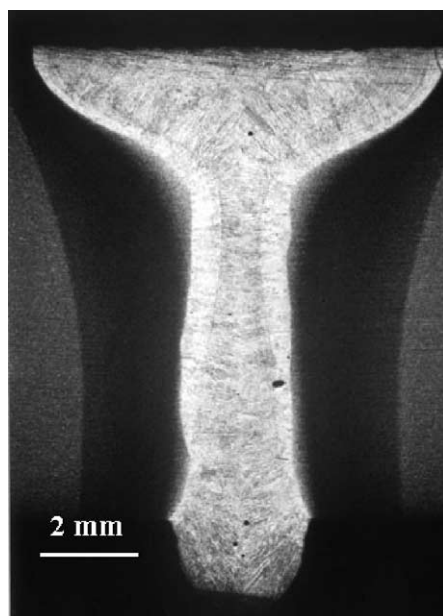


Fig. 7. Macrograph of a Eurofer plate laser weld, 9 mm thick.

passes. Lack of fusion was achieved by decreasing the current and tilting the torch at 45° (see Fig. 9); porosity was achieved by drilling. The samples were HIPed at 1100 °C, 100 MPa and it was shown by X-ray detection that both defects disappeared during HIP.

#### 4. Manufacturing technologies for the HCPB blanket breeder and neutron multiplier

##### 4.1. Ceramic tritium breeder

##### 4.1.1. Ortho-silicate

Li<sub>4</sub>SiO<sub>4</sub> pebbles with natural <sup>6</sup>Li-enrichment (7.5 at.%) and a slight surplus of SiO<sub>2</sub>, are produced by melting a mixture of Li<sub>4</sub>SiO<sub>4</sub> and SiO<sub>2</sub> powders at about 1450 °C in a container made of Pt-alloy, then spraying



Fig. 8. Microstructure of the weld zone, Eurofer TIG weld.

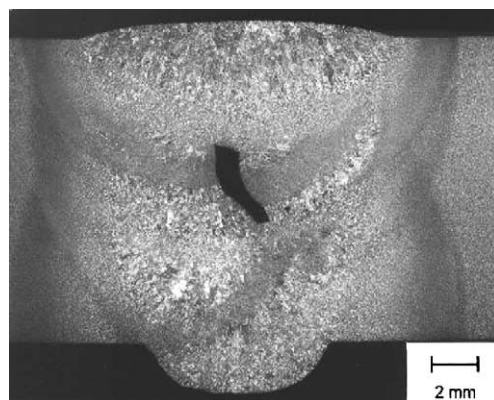


Fig. 9. Intentional lack of fusion defect in 14 mm thick Eurofer weld (macrography).

Table 4

Tensile properties of Eurofer TIG weld, 24 mm thick, after PWHT at 740 °C, 2.5 h

| Location orientation  | Root         |      |             |      | Middle       |      |             |      | Top          |      |             |      |
|-----------------------|--------------|------|-------------|------|--------------|------|-------------|------|--------------|------|-------------|------|
|                       | Longitudinal |      | Transversal |      | Longitudinal |      | Transversal |      | Longitudinal |      | Transversal |      |
| Temperature (°C)      | 20           | 400  | 20          | 400  | 20           | 400  | 20          | 400  | 20           | 400  | 20          | 400  |
| $\sigma_y$ (MPa)      | 643          | 566  | 716         | 568  | 710          | 553  | 726         | 577  | 727          | 564  | 685         | 576  |
| $\sigma_{max}$ (MPa)  | 749          | 589  | 787         | 591  | 803          | 575  | 794         | 600  | 822          | 605  | 786         | 594  |
| Elongation (%)        | 14.7         | 13.9 | 14.6        | 12.1 | 14.8         | 16.6 | 14.6        | 8.3  | 15.0         | 8.8  | 15.1        | 10.7 |
| Reduction of area (%) | 54.4         | 44   | 50.8        | 35.5 | 53.3         | 35.2 | 53.6        | 32.7 | 49.6         | 41.8 | 50.7        | 20.3 |

Specimens machined from the weld zone, means values over 3 specimens.



the liquid in air, and afterwards sieving the solidified sprayed material in form of pebbles. Pebbles having diameter in the range 0.25–0.63 mm are selected for the use as breeder blanket material. In case of  $^6\text{Li}$  enriched  $\text{Li}_4\text{SiO}_4$  pebbles, a mixture of  $\text{Li}_4\text{SiO}_4$ ,  $\text{SiO}_2$  and  $^6\text{Li}$ -enriched  $\text{Li}_2\text{CO}_3$  is melted and sprayed. As enriched lithium orthosilicate powder is not available on the market, highly enriched lithium carbonate powder is used and pebbles with the needed  $^6\text{Li}$ -enrichment can be obtained by mixing  $\text{Li}_2\text{CO}_3$  with  $\text{Li}_4\text{SiO}_4$  (to dilute the  $^6\text{Li}$  percentage in the mixture) and  $\text{SiO}_2$  powders. A new promising method is being developed using  $\text{LiOH}$  powder for both enriched and non-enriched pebbles. The lithium orthosilicate pebbles produced from lithium hydroxide so far showed very good characteristics [20].

#### 4.1.2. Meta-titanate

The main reference steps for the production of  $\text{Li}_2\text{TiO}_3$  pebbles are: the preparation of the  $\text{Li}_2\text{TiO}_3$  powder by blending  $\text{Li}_2\text{CO}_3$  and  $\text{TiO}_2$  powder, the pasting with a binder and plasticiser, the extrusion and cutting in granules, the shaping by spheronisation and the final sintering.

The quality of the final sintered pebbles depends on the characteristics of the intermediate products. They can be varied in a wide range by adjusting the fabrication parameters. This is a significant advantage of the process as it allows tailoring the  $\text{Li}_2\text{TiO}_3$  pebbles properties and, hence, the pebble bed behaviour.

The EU is also investigating the possibility of a production and recycling (for the recovery of enriched Li) method using a direct wet process [21]. Encouraging results have been obtained but the process is still under development in collaboration with Japanese researchers.

#### 4.2. Beryllium neutron multiplier

In the HCPB beryllium (Be) is in the form of pebbles. Beryllium pebbles have been produced since the beginning of the 90's by rotating electrode process (REP). A high-purity beryllium electrode melts in an arc ejecting droplets, which solidify in a helium atmosphere. The reference Be pebbles are 1-mm diameter. The chosen diameter is obtained by controlling the rotation speed of the electrode. The pebbles (Fig. 10) are produced with an optimised composition to avoid the formation of low temperature melting impurity phases at grain boundaries which might enhance swelling [22].

In 2002 a critical re-assessment of the reference material was carried out in order to improve the swelling and tritium inventory properties. The EU R&D effort is presently investigating the use of small grain Be pebbles. Extrapolating theoretical predictions by the ANFIBE code ideal grain sizes to have a practically complete gas release would be less than 1  $\mu\text{m}$ , which cannot be obtained by the REP method. In order to produce pebbles

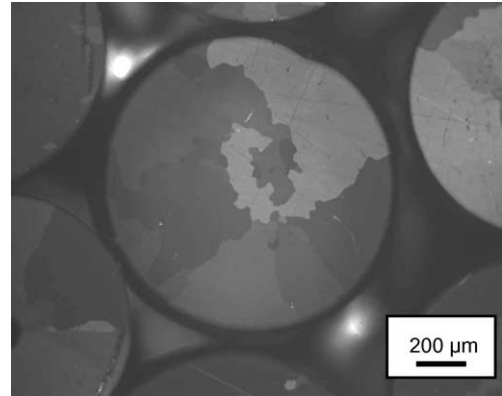


Fig. 10. Microstructure of the EU reference beryllium pebbles.

with such microstructure starting from powder, a pilot R&D activity has been started in FZK; at the same time, Be disks with such microstructure, produced at Bochvar institute in Moscow, will be characterised also after an irradiation campaign in the HFR reactor in Petten with production of up to 6000 appm helium.

## 5. Conclusions

The basic manufacturing technologies for the construction of the TBMs have been selected and are being developed in the EU. HIP has been chosen as the main manufacturing technique for the main substructures of the TBM and fusion welds are used for assembling the main parts. In parallel the production processes for the breeder and neutron multiplier have been defined and tested. R&D results have confirmed the suitability of the selected technologies for the HCPB and HCLL BB designs and have given confidence for starting the construction of the large-scale prototypical mock-ups of the TBMs, which are the last step in development before the final manufacturing of the first TBMs, which will be installed and tested in ITER.

## References

- [1] L. Boccaccini, L. Giancarli, G. Janeschitz, S. Hermesmyer, Y. Poitevin, A. Cardella, E. Diegele, J. Nucl. Mater., these Proceedings. doi:10.1016/j.jnucmat.2004.04.125.
- [2] S. Hermesmyer, J. Fiek, U. Fischer, C. Köhly, S. Malang, J. Rey, Z. Xu, in: Proceedings of SOFE-20, San Diego, CA, 2003.
- [3] A. Li Puma, Y. Poitevin, W. Farabolini, J. Szczepanski, Helium cooled lithium lead blanket module for DEMO. Design and analyses, CEA/Report, CEA/Saclay, SERMA/LCA/RT/03-3297, September 2003.
- [4] R.L. Klueh, D.S. Gelles, S. Jitsukawa, A. Kimura, G.R. Odette, B. van der Schaaf, M. Victoria, J. Nucl. Mater. 307–311 (2002) 455.

- [5] B. van der Schaaf, F. Tavassoli, C. Fazio, E. Rigal, E. Diegele, R. Lindau, G. Le Marois, *Fusion Eng. Des.* 69 (1–4) (2003) 197.
- [6] R. Lindau, M. Schirra, *Fusion Eng. Des.* 58&59 (2001) 781.
- [7] R. Lindau, A. Möslang, M. Schirra, *Fusion Eng. Des.* 61&62 (2002) 659.
- [8] T. Lechler, H.-J. Fiek, S. Gordeev, K. Schleisiek, *Fusion Eng. Des.* 49&50 (2000) 585.
- [9] E. Rigal, G. Le Marois, T. Lechler, G. Reimann, K. Schleisiek, L. Schäfer, P. Weimar, *Fusion Eng. Des.* 49&50 (2000) 651.
- [10] K. Schleisiek, T. Lechler, L. Schäfer, P. Weimar, *J. Nucl. Mater.* 283–287 (2000) 1196.
- [11] A. Danón, A. Alamo, *J. Nucl. Mater.* 307–311 (2002) 479.
- [12] K. Furuya, E. Wakai, M. Ando, T. Sawai, A. Iwabuchi, K. Nakamura, H. Takeuchi, *Fusion Eng. Des.* 69 (2003) 385.
- [13] P. Norajitra, G. Reimann, R. Ruprecht, L. Schäfer, *J. Nucl. Mater.* 307–311 (2002) 1558.
- [14] W. Dietz, A. Alamo, R. Lindau, Technical specification, supply of RAFM steel type 9CrWTaV, NET 97/917, July 1997.
- [15] A. Fontes, *Fusion Technology Annual Report of the Association EURATOM/CEA 2001*, p. 267.
- [16] P. Aubert, P. Peyre, *Fusion Technology Annual Report of the Association EURATOM/CEA 2001*, p. 417.
- [17] L. Forest, *Fusion Technology Annual Report of the Association EURATOM/CEA 2002*, p. 193.
- [18] L. Forest, *Fusion Technology Annual Report of the Association EURATOM/CEA 2002*, p. 175.
- [19] L. Forest, *Fusion Technology Annual Report of the Association EURATOM/CEA 2002*, p. 189.
- [20] W. Pannhorst, V. Geiler, G. Räke, B. Speit, D. Sprenger, in: *Proceedings of 20th Symposium on Fusion Technology*, Marseille, France, 7–11 September 1998.
- [21] K. Tsuchiya, M. Uchida, H. Kawamura, S. Casadio, C. Alvani, in: *Proceedings of the 10th International Workshop on Ceramic Breeder Blanket Interactions*, Karlsruhe, Germany, 2001.
- [22] G. Piazza, in: W. Bahm (Ed.), *Nuclear Fusion Programme Annual Report of the Association Forschungszentrum Karlsruhe/EURATOM*, October 2000–September 2001, Report FZKA 6650/EUR 20162 EN, Forschungszentrum Karlsruhe, 2002.